

GNC DESIGN AND VALIDATION FOR RENDEZVOUS, DETUMBLING, AND DE-ORBITING OF ENVISAT USING A CLAMPING MECHANISM

*J. F. Vasconcelos⁽¹⁾, M. Kerr⁽²⁾, P. Rosa⁽¹⁾, M. Hagenfeldt⁽²⁾, A. Fabrizi⁽²⁾,
B. Parreira⁽¹⁾, J. Ambrósio⁽³⁾, M. Casasco⁽⁴⁾, and G. Ortega⁽⁴⁾*

⁽¹⁾ Deimos Engenharia, Lisbon, Portugal. Contact: jose.vasconcelos@deimos.com.pt

⁽²⁾ Elecnor Deimos, Tres Cantos, Spain. Contact: murray.kerr@elecnor.es

⁽³⁾ IDMEC, Instituto Superior Técnico, Lisbon, Portugal. Contact: jorge@dem.ist.utl.pt

⁽⁴⁾ ESTEC, ESA, Noordwijk, Netherlands. Contact: massimo.casasco@esa.int

ABSTRACT

This paper describes the development and validation of a GNC for active debris removal (ADR) of the ENVISAT S/C, using a clamping mechanism. The GNC design is focused on the phases where the choice of a clamp mechanism is of particular relevance to the ADR execution, namely final pre-capture rendezvous with uncooperative target, post-capture detumbling and stabilization of the composite, and de-orbiting. The derived GNC solutions are based on robust MIMO control, explicitly considering the dynamics of the chaser, target, clamp attachment, flexible appendages and sloshing effects. Also, the solution is designed to be robust to exogenous disturbances, and to uncertainties in the mass, center-of-mass and inertia (MCI) parameters, among others. An advanced verification and validation framework for GNC is also exploited, stemming from the μ -synthesis framework, providing analytical performance and stability characterization of the system. Supplementary validation results are obtained from a Monte-Carlo campaign. The GNC results obtained in this work support the consolidation of a set of requirements for future missions, especially those within ESA's CleanSpace initiative.

Index Terms— Active Debris Removal (ADR), Guidance Navigation and Control (GNC), Robust control, Multi-body systems, Analytical validation.

1. INTRODUCTION

ESA and the European space industry have recently embarked on the so called CleanSpace initiative [1] headed towards establishing a European capability for de-orbiting and/or re-orbiting to a graveyard orbit of Space Debris. Such capability would enable the disposal in the future of the required number of objects with the long-term goal of stabilizing the population of Space Debris.

e.Deorbit is an ADR study developed by ESA in the context of the CleanSpace initiative [2]. Its main objective is to produce a preliminary system design for the most promising capture mechanisms, identifying the technology roadmap and considering its applicability to other ESA

missions. The study is focused on two categories of mechanisms: rigid links (e.g. robot arm, tentacles) and flexible links (e.g. net, tether gripper, harpoon).

CLGADR is a study for the development of ADR GNC in the scope of e.Deorbit, focused on the phases where the choice of the clamp mechanism is of particular relevance to the ADR execution [3], i.e. those starting immediately before capture, and ending on the actual de-orbiting of the target.

This paper describes the development and validation of the ADR GNC, based on robust MIMO control, for capture and de-orbiting of an uncooperative target. The results of the GNC design activities are presented, namely regarding: the multi-body modeling of the chaser and composite S/C, the Linear Fractional Transformation (LFT) modeling of the plant dynamics for GNC synthesis, and the GNC architecture and subsystems design. Validation of GNC robustness is obtained analytically within an advanced verification and validation framework, based on μ -synthesis tools. In addition, numeric validation is performed in a high-fidelity simulator of S/C dynamics, including multi-body dynamics, flexible modes, sloshing, MCI perturbation, environmental disturbances, among others. The obtained GNC results allow for the consolidation of a set of requirements, relevant for future missions with uncooperative targets.

The structure of the paper is based on the sequence of GNC development activities, as follows. Section 2 defines the mission scenario and presents the main requirements driving the GNC design. Section 3 presents the main models supporting GNC development, namely the multi-body dynamics of the mission scenario, and the LFT models for robust control synthesis. The GNC development is presented in Section 4 and Section 5, respectively for pre- and post-capture phases, covering GNC architecture and modes definition, and GNC sub-system design and implementation. The advanced validation framework is presented in Section 6, describing the analytical and simulation tools considered in ADR GNC validation. The obtained validation results and their analysis is presented in Section 7. A concluding summary of the work is found in Section 8.

2. MISSION DEFINITION AND REQUIREMENTS

This section presents the main aspects of the mission definition, and summarizes the requirements driving the GNC design and validation.

2.1. Mission phases and scenarios

The mission phases considered in the study are illustrated in Figure 1 and described in the following.

- **Pre-Capture Phase**, described by a final rendezvous towards a capture configuration. This phase starts at a station keeping point (SK), followed by the acquisition of co-rotation (also denoted as synchronous station keeping, SSK) to attain null velocity w.r.t. the target. It is finalized by a forced approach to reach a capture distance w.r.t. target body, while keeping co-rotation.
- **Target Stabilization Phase**, defined immediately after the connection has been achieved between both S/C. In this phase, the chaser detumbles the target, nullifying its angular velocity, and rotates the composite to attain the attitude pointing required for de-orbiting;
- **Stack Orbit Transfer and Disposal Phase**, defined as the phase where the de-orbiting of the composite is performed, using a gradual perigee lowering strategy.

The target S/C is ENVISAT, being considered uncooperative for the purpose of the ADR mission [2]. The GNC is designed to operate for any of three following rotational scenarios of ENVISAT:

- Nominal scenario, derived from E-deorbit mission studies [5], and defined by a 3.5 deg/s angular velocity aligned with H-bar and with the target's y-axis, see Figure 1;
- Two alternative scenarios, defined by a worst-case 5 deg/s angular velocity, being LVLH fixed in one scenario and inertially fixed in the other.

The developments presented in this paper address the nominal scenario; the GNC results and sensitivity analysis for the alternative scenarios is omitted, due to space constraints.

2.2. GNC requirements

The ADR GNC is subject to requirements that can be organized in three categories: design, robustness, and performance. A summary of the requirements in each category is presented in the following.

The **design requirements** specify aspects such as the GNC design method, objectives, and general characteristics, and hence are assessed by review of design. The design requirements considered in the study state that the GNC must:

1. Use modern MIMO robust techniques that provide analytical stability characterization and, by design, can cope with uncertainties in the model;
2. Be autonomous (using ground only for high-level decisions) and generic (with respect to orbit radius);

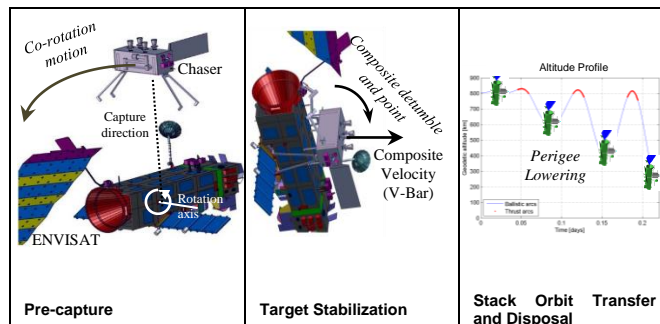


Figure 1 – Mission phases considered in GNC design.

3. Match the target rotation during final approach, such that relative velocity is null;
4. Attain a final capture relative distance that is constant and between 2m and 3m point-to-point;
5. For pre-capture, control the position, velocity, attitude and attitude rate of chaser (6-DoF) relative to the target;
6. For post-capture, control the attitude of the composite chaser-clamp-target during stabilization and de-orbiting.

The **robustness requirements** specify the effects that the GNC must be robust to, and quantify the closed-loop stability criteria, e.g. μ and modulus margin. In the adopted robust control framework, these requirements are considered explicitly in the design of the GNC, and validated analytically using robust control tools. The robustness requirements can be summarized as follows:

1. The GNC must be robust to the following effects:
 - All significant modeled sensor and actuator errors;
 - Sloshing and flexible modes of both S/C;
 - Air-drag (which is the most significant exogenous disturbance at lower altitudes of de-orbiting);
 - Discontinuities due to de-orbiting thruster step function;
 - ENVISAT slippage up to 0.1m w.r.t. chaser during de-orbit boosts.
2. The GNC must satisfy the following stability criteria:
 - Structured singular value such that $\mu < 1$;
 - Modulus margin larger than -6dB.
3. The GNC must be robust against the uncertainties presented in Table 1.

The **performance requirements** quantify the errors of the GNC in tracking the desired profile. For pre-capture, they specify the accuracy of positioning and pointing at SK and at SSK. For post-capture, they specify the attitude and angular velocity errors after target stabilization and during de-orbit burn. The performance requirements were formulated and matured in the course of the study, and their final form is found in the validation results of Section 7.

Table 1 – Mission scenario uncertainties (3σ).

Parameter	Chaser S/C	Target S/C
Mass	$\pm 5\%$	$\pm 0.2\%$
Inertia	$\pm \begin{bmatrix} 10 & 20 & 20 \\ 25 & 10 & 20 \\ 10 & 20 & 10 \end{bmatrix} \%$	$\pm \begin{bmatrix} 2.0 & 25 & 11.5 \\ 25 & 2.4 & 43.4 \\ 11.5 & 43.4 & 2.3 \end{bmatrix} \%$
CoM	$\pm 0.1\text{m}$	$\pm 0.01\text{ m (until de-orbit)}$ $\pm 0.10\text{ m (during de-orbit)}$
Flexible modes	$\pm 20\%$ in damping ratio $\pm 20\%$ in frequency	

3. MODELING

This section presents the models considered in the development of the ADR GNC, as follows. Section 3.1 describes the multi-body dynamics framework used to obtain the analytical models covering all the elements of mission scenario (chaser, target, clamp, flexible appendages, sloshing, etc.). These models are inherently complex and non-linear, and their purpose is two-fold: to be implemented in the high-fidelity simulator, so that closed-loop GNC results are obtained in a representative environment; to be a reference in the derivation of the LFT models presented in Section 3.2. These LFT models are a key element in the control synthesis, allowing the robust control tools to obtain a controller that has stability and performance robustness for the plant dynamics and uncertainties modeled in the LFT.

3.1. S/C and Clamping Mechanism Multi-body Dynamics

The general concept of a rigid body with a flexible appendage used in this work is given by the equations of motion for the linear elastic flexible body [6], where the flexible generalized coordinates are the local nodal coordinates associated to the finite element discretization of the flexible body. A component mode synthesis technique is adopted to reduce considerably the number of generalized coordinates associated with flexible modes, increasing the computational efficiency. The resulting number of generalized coordinates is equal to the number of modes considered, added to the position and attitude coordinates of the rigid body.

The clamping mechanism is modeled by considering a discrete number of clamping points in the face of each S/C; the exchange of forces between the S/C is modeled through a classic penalty approach. The flexible clamping interface is designed through Kelvin-Voigt spring-damper systems, linking each pair of clamping points. The mechanical model for the clamping mechanism is achieved via a collection of unilateral springs and dampers, describing the axial resistance of the four rod (traction), the axial effect of the two arms (compression) and the transversal resistance of the four pushing rods (bi-directional).

This modeling strategy allows to assess in simulation the clamping mechanism properties, namely:

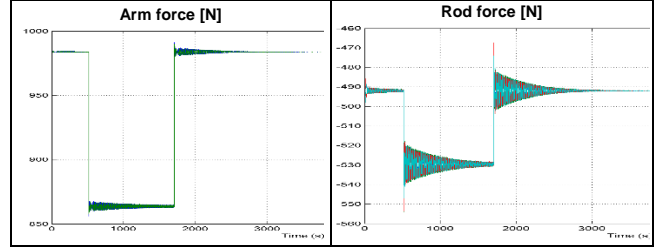


Figure 2 – Clamp mechanism forces during de-orbit boost.

- the joint reaction forces, Figure 2, showing that the reaction forces operate always in the elastic range, maintaining the clamping of the mechanism;
- the natural frequency of the mechanism, both in the axial and transversal directions, showing that these match the expected theoretical values.

The sloshing motion has been taken into account as well, with the dynamics of the fluid being described by a mechanical model in the form of a spring-mass system [7]. The effect of fuel consumption is also considered, namely during de-orbiting phase, by considering a step-wise fuel consumption, with a sloshing model parameterization dedicated to each de-orbit burn.

3.2. LFT models

An LFT model is a representation of a linear system consisting in the feedback connection (see Figure 3) of a linear time invariant plant $M(s)$ and a block diagonal matrix $\Delta(s)$ containing real- or complex-valued parameters representing the uncertain/time-varying/nonlinear part of the model. In this study, the LFT models encompass the elements specified in the robustness requirements, so that, by design, the resulting controller has the desired stability and performance robustness.

For **pre-capture**, the derived LFT considers:

- the relative position and velocity dynamics of the chaser, described by the Yamanaka-Ankersen equations [4];
- the attitude and angular rate error dynamics with respect to the reference trajectory;
- the flexible modes and sloshing dynamics, described by linear systems [4] complemented by $\Delta(s)$ to shape the uncertainties in the flexible elements, see Table 1;
- the MCI uncertainties of the chaser, see Table 1;
- the disturbance in the measurements and in the actuation, and the state estimation error.

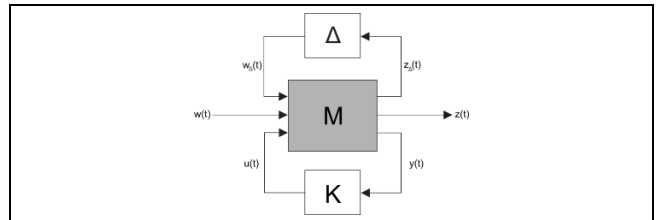


Figure 3 – LFT and control synthesis framework.

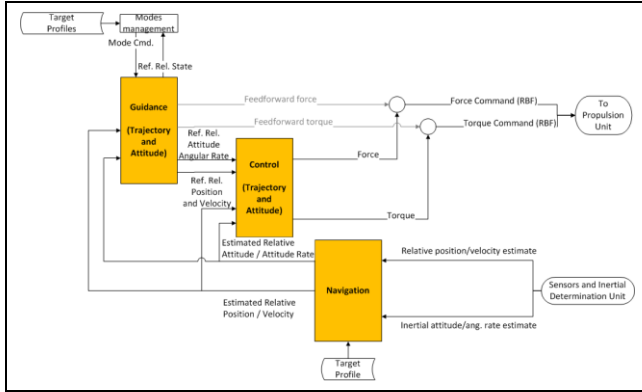


Figure 4 – GNC block diagram for pre-capture phase.

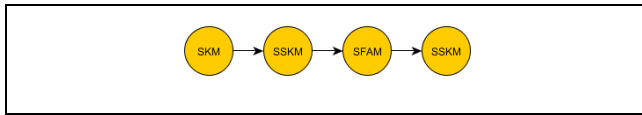


Figure 5 – Pre-capture GNC mode transition.

For **post-capture**, the LFT is derived by adapting the non-linear multibody dynamics of Section 3.1, delivering a state-space description of the plant that is a compromise between the accuracy of complex nonlinear models, and the numerical treatability required for the well-established controller synthesis techniques for linear systems [5].

Post-capture control is focused on attitude control for stabilization of the composite and for pointing during de-orbiting. Consequently, the LFT model considers:

- the chaser attitude and angular rate error dynamics with respect to the reference trajectory frame;
- the position, velocity, attitude and angular velocity of target with respect to the chaser;
- the forces of the clamping mechanism and the related torques;
- the MCI uncertainties of both S/C and the ENVISAT slippage during de-orbit burns, see Table 1;
- the flexible modes of both S/C and sloshing dynamics of the chaser, described by LTI systems [4] and complemented by $\Delta(s)$ to shape the uncertainties in the flexible elements, see Table 1;
- the disturbance in the measurements and in the actuation, and the chaser inertial state estimation error.

4. PRE-CAPTURE DESIGN

This section presents the development of the GNC for the pre-capture phase, describing the GNC architecture, and the synthesis of the GNC sub-systems.

4.1. GNC Modes and Architecture

The set of GNC modes is defined by considering the mission phases and GNC requirements presented in Section 2. The

modes for the pre-capture phase are presented in the sequel, and the mode transition is depicted in Figure 5:

- **Station Keeping Mode (SKM)**: the first mode of pre-capture maintains the S/C at a relative position and attitude that are fixed in LVLH, counteracting natural dynamics and/or perturbations;
- **Synchronous Station Keeping Mode (SSKM)**: this mode acquires and maintains a S/C position and attitude that are fixed w.r.t. the target, describing a forced co-rotation motion. As shown in Figure 5, this mode is commanded at two points: after SK, to acquire co-rotation; after synchronous forced approach, to maintain co-rotation at capture distance;
- **Synchronous Forced Approach Mode (SFAM)**: this mode performs the forced approach to acquire capture distance w.r.t. target. It is executed between SSK at initial distance, and SSK at capture distance, performing a transition between both distances.

In all of the aforementioned modes, the GNC functions are active, fully autonomous, and command 6-DoF control thrusters. The GNC architecture for pre-capture is shown in Figure 4. The operations associated with each GNC subsystem are the following:

- **Guidance** function is tasked with providing the reference trajectory to the controller, namely considering solutions of the relative dynamics [4];
- **Control** covers both the relative attitude and translational control problems;
- **Navigation** estimates the relative state between chaser and target, considering the model of the relative dynamics and the relative sensor measurements. Due to the focus of the study in robust control design, the estimation function takes the form of a performance model.

4.2. Guidance Design

This section describes the Guidance design, focusing on the derivation of the approach profile for the nominal scenario of Section 2.1. The derivation was obtained satisfying the following non-relaxable constraints:

- the approach direction, given by the z-axis of the target, is rotating in LVLH, see Figure 1, and hence requires the chaser to perform co-rotation at capture;
- the SK must have a distance such that the ENVISAT will not collide with the chaser;
- the angular rate of the target must be tracked by the chaser in SSK. Therefore, the thrust authority must suffice to acquire and maintain SSK;
- the chaser must keep the target within the FoV.

Given these constraints, the derived approach profile is shown in Figure 6, being defined by the following sequence of events:

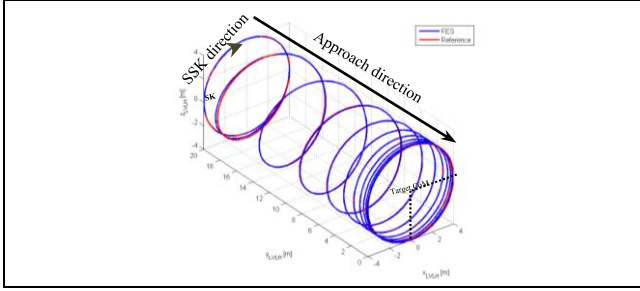


Figure 6 – Close-range rendezvous profile in LVLH.

1. Perform SK at $p_{SK} = [-r_{CR} \ d_1 \ 0]$ in LVLH, where d_1 is the SK distance along H-bar and r_{CR} is the co-rotation radius;
2. Acquire co-rotation, described by the position in LVLH $p(t) = [r_{CR} \cos(\omega_{CR}t) \ d_1 \ -r_{CR}\sin(\omega_{CR}t)]$, where ω_{CR} is the co-rotation angular rate, e.g. 3.5 deg/s for nominal scenario;
3. Command a passively safe forced approach profile [8] along H-bar, to simultaneously reduce d_1 towards the origin, and to drive the value of r_{SK} towards the capture distance, thus acquiring the capture configuration.

4.3. Control Design

This section describes the MIMO robust controller design for the pre-capture phase. From the mission definition and requirements of Section 2, the main controller objectives are set to regulate the S/C translational and rotational states, and to command the spacecraft actuators, taking as inputs the navigation solution and guidance commands. Also, the pre-capture controller must satisfy, by design, the robustness requirements of Section 2.2.

The overall controller synthesis methodology can be structured into the following three steps:

- **Modeling:** The derivation of a reliable model is of paramount importance for control design. The model adopted is described by the LFT presented in Section 3.2;
- **Controller design/synthesis:** this step is where the controller is actually computed. A key point is the proper definition of the dynamic weights, which are used to shape the frequency response of the closed-loop system;
- **Analysis:** The closed-loop system is evaluated using analytical tools available in robust control methodology, assessing the robustness properties of interest.

The controller synthesis scheme considered is depicted in Figure 3. To attain the desired stability and performance robustness, the controller is synthesized with complex-valued model uncertainty, as well as uncertain parameters. An iterative, performance- and robustness-guided approach to the H_∞ unstructured control design was adopted. This approach enabled addressing numerical issues due to the particularly large LFT model, for which the mixed- μ D,G-K iterations [9] could not be effectively implemented.

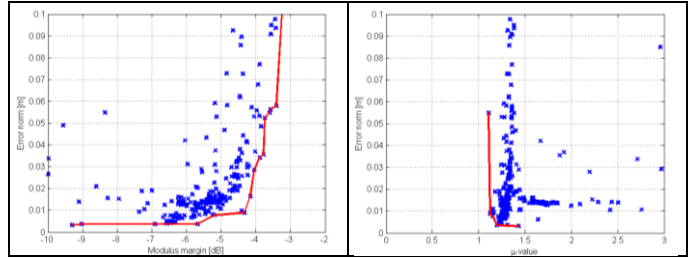


Figure 7 – HDE optimization results: SSK position norm error vs modulus margin [left] and μ value [right].

Instead, the strategy adopted was to tune the dynamic weights of the augmented plant, by using a global optimization algorithm, referred to as Hybrid Differential Evolution (HDE) [13].

Another relevant technique adopted is the so-called *two degrees-of-freedom* controller. In addition to having the tracking error as an input, this controller also has direct access to the Guidance reference. The controller thus synthesized will, by design, output a feed-forward (FF) term that not only improves the system performance, but also explicitly takes into account model uncertainty and exogenous disturbances. Unlike the classical FF terms, the obtained term inherits the robustness guarantees of modern robust control.

The results from the controller synthesis are summarized in Figure 7, where each blue cross represents the controller obtained for a specific set of weights. The red thick line is the Pareto optimal set, i.e., the points with best performance for given stability/robustness (modulus margin, μ -value). This line illustrates the tradeoff between performance and stability/robustness and, with respect to the considered scenario, shows that there exists a control solution satisfying the robustness and performance requirements.

5. POST-CAPTURE DESIGN

This section presents the development of the GNC for the post-capture phase, describing the GNC architecture, and the synthesis of the GNC sub-systems.

5.1. GNC Modes and Architecture

The set of GNC modes is defined by considering the mission phases and GNC requirements presented in Section 2. The modes for the post-capture phase are presented in the following, and the mode transition is depicted in Figure 9:

- **Composite Stabilization Mode (CSM):** the first mode of post-capture smoothly cancels the composite angular velocity in LVLH;
- **Composite Pointing Mode (CPM):** this mode steers the composite towards a specific constant direction in LVLH;
- **Composite Disposal Mode (CDM):** this mode performs the de-orbiting trajectory. De-orbit burns are applied by a dedicated main engine. This mode is semi-autonomous,

having the desired delta-V and timeline specified by ground. Sub-modes are:

- (W)ait: monitor the S/C orbit evolution;
- (O)rientation: fine point the composite in LVLH;
- (B)oost: apply the de-orbiting boost at apogee;
- Post-Boost Stabilization (PBS): stabilize attitude subsequently to the deactivation of the main engine.

In all of the aforementioned modes, the GNC functions are active, fully autonomous, and command 3-DoF control thrusters, except where otherwise stated. The GNC architecture for post-capture is shown in Figure 8. The operations associated with each GNC subsystem are designed to regulate attitude in LVLH, and to command de-orbit burns timely as follows:

- **Guidance** provides attitude reference for each mode. At CDM, Guidance commands the boosts at the specified time instant, for perigee lowering;
- **Control** covers the attitude control problem, using 3 DoF torque control authority. At CSM and CPM, the control focuses on the stabilization of the stack chaser-clamp-target, and subsequent pointing. At CDM, the controller accurately points the composite for proper application of the de-orbiting ΔV ;
- **Navigation** provides measurements of the chaser attitude (for attitude control) and chaser position and velocity (for monitoring of CDM). Due to the focus of the study in robust control, the inertial position and attitude estimate are provided by performance models of estimation units.

It is remarked that the controller is designed to stabilize the composite, but navigation only provides information regarding the chaser. This implies that the controller has to regulate states that are not directly known, e.g. the attitude and position of the target w.r.t the chaser, that are time-varying due to the clamp connection flexibility. The synthesis of such a controller is one of the benefits of using MIMO H_∞ control theory.

5.2. Guidance Design

This section describes the main aspects of Guidance design. The Guidance functionality for each GNC modes is the following:

- **CSM:** Guidance outputs a null angular velocity in LVLH. This implies that the controller will stabilize the angular velocity along a suitable multi-axis direction, instead of a sequential stabilization, e.g. Yaw, Pitch and Roll axes. This solution is enabled by the MIMO framework, which naturally considers the coupling between axes;
- **CPM:** Guidance considers the initial attitude and returns an attitude profile that smoothly drives the attitude towards the desired configuration of V-bar pointing;
- **CDM:** Guidance monitors the time elapsed to switch between sub-modes. The reference attitude and angular

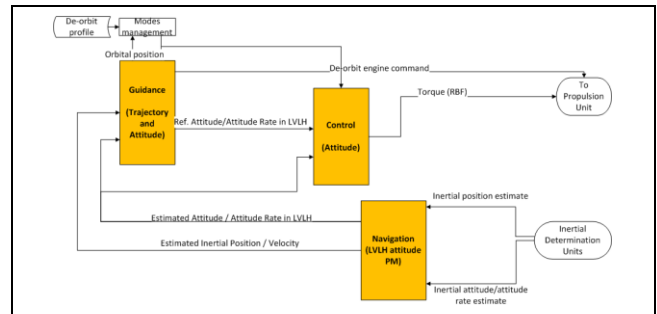


Figure 8 – GNC block diagram for post-capture phase.

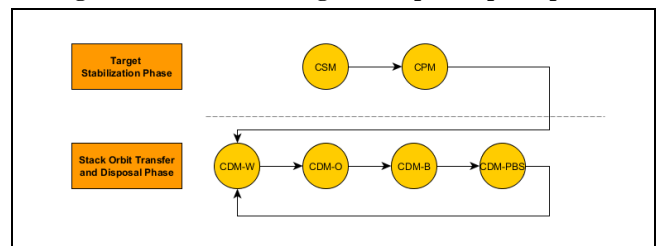


Figure 9 – Post-capture GNC mode transition.

velocity are commanded such that V-bar pointing is obtained. Main engine burns are applied in CDM-B;

The de-orbiting profile to be followed was also defined in the study, given the following guidelines:

- must be a multiple fixed-magnitude burn profile for gradual perigee lowering;
- the duration of the boosts should be less than 20% of orbit period, and the final perigee altitude should be 60km [10];
- the main engine for de-orbit boosts has a nominal thrust authority of 450N.

The degrees of freedom in the design of the profile are the number of de-orbiting burns, and the intermediate perigee altitudes. The resulting profile is composed of 4-burn manoeuvres around apogee, with the total predicted delta-V is 216 m/s, corresponding to a fuel consumption of 606.5 kg.

5.3. Control Design

This section describes the MIMO robust controller design for the post-capture phase. From the mission definition and requirements of Section 2, the main controller objectives are set to regulate the composite rotational state, and to command the spacecraft torque actuators, taking as input the navigation estimates and guidance reference.

The controller synthesis methodology and scheme are those previously defined in Section 4.3, and depicted in Figure 3. The synthesis is obtained for the LFT described in Section 3.2, and therefore considers explicitly the coupled multi-body dynamics of the S/C ensemble, including clamping mechanism, sloshing and flexible modes. The H_∞ and real/mixed- μ approaches were exploited, and the adopted the controller satisfied, by design, the robustness requirements of Section 2.2.

Although a common control synthesis method is adopted for all modes, CSM and CPM have distinct performance requirements. Dedicated controllers are synthesized for each mode, using specific design weights, as follows:

- **CSM:** The objective is to dissipate the high rotational kinematic energy of the composite, so the controller shall penalize the angular velocity error. Actuation is also penalized as necessary to keep the actuation signals within the saturation limits;
- **CPM, CDM:** The objective is to drive and maintain the composite in V-bar pointing, so the controller penalizes attitude error. In CPM, the controller transitions from the initial to the desired attitude by tracking a smooth attitude reference generated by Guidance; in CDM, the same controller tracks the desired V-bar pointing.

6. VALIDATION FRAMEWORK

This section summarizes the analytical and simulation-based tools adopted in ADR GNC validation. Section 6.1 presents the modern control tools that enable theoretical analysis of the stability and performance robustness of the GNC algorithm. Section 6.2 presents the MIL simulation framework, developed for performance assessment of the GNC concept for the composite system, supporting GNC and mission trade-offs.

6.1. Analytical Validation Tools

Robust control techniques provide tools such as μ -analysis, that characterizes closed-loop stability and performance with robustness considerations, i.e. the obtained analysis is valid for the nominal system and for all the acceptable realizations of the uncertain parameters [9]. The characterization is provided by the computation of structured singular value μ bounds: if the upper bound is smaller than one, then closed-loop stability and performance is ensured for all admissible realizations of the uncertainties; if the lower bound is greater than one, then the closed-loop can be destabilized by some realizations, that can be determined numerically.

In the case of CLGADR, the analytical validation has the following main benefits:

- provides an assessment of the robustness requirements of Section 2.2, that is valid irrespectively of validation in simulation. Consequently, the dependency on Monte-Carlo (MC) campaigns for requirement assessment is reduced;
- provides explicitly worst-case conditions for stability and performance. Among other applications, these conditions can be replicated in simulation, for further insight;
- guarantees a given modulus margin for the closed-loop system.

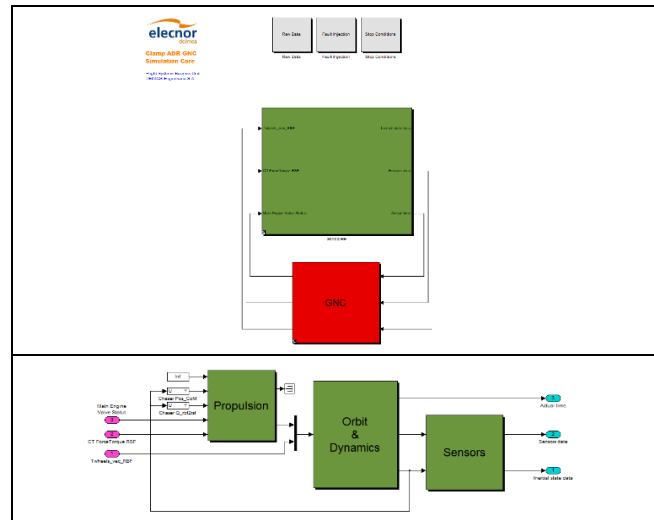


Figure 10 – CLGADR MIL Simulator [top] and SIMCORE block [bottom].

The analytical tools are valid under the assumption that the LFT model accurately captures the behavior of the nonlinear plant. Therefore, the results of analytical validations are admissible under the assumptions adopted in the LFT derivation. The GNC validation for the comprehensive non-linear model is obtained by time-domain MC campaign, assessing the validity of the LFT assumptions, and illustrating the stability and performance robustness in the time-domain.

6.2. MIL Simulation Framework

The design and validation of the GNC was supported by the development of a Model-in-the-loop (MIL) simulator for ADR missions, implemented in Matlab and Simulink. The MIL is a maturation of Deimos background experience in simulation environments for rendezvous projects [11] [12], extended with new models in the frame of CLGADR.

The MIL, illustrated in top of Figure 10, is a high-fidelity simulation environment, including dynamics of the chaser and target for pre-capture, and the multi-body dynamics of both S/C connected by a clamping mechanism for post-capture. The SIMCORE block, shown in bottom Figure 10, also encompasses flexible modes, sloshing dynamics, environmental disturbances, and representative sensors and actuators models, including associated non-idealities. The MIL is designed for easy setup of the several mission configurations considered, namely those related to the S/C dynamics (single and multi-body); the ENVISAT rotation scenario; the dynamics of the S/C appendages (flexible modes, sloshing); the relative sensor performance; among others. The MIL has a MC campaign mode that applies dispersion to all the parameters considered in the study requirements, for multiple simulation shots.

7. VALIDATION RESULTS

This section presents the analytical and simulation-based validations of the ADR GNC, obtained using the verification and validation (V&V) framework previously described.

7.1. Analytical Validation Results

7.1.1. Pre-capture validation

For pre-capture, the results for robust stability and performance of μ -analysis are depicted in Figure 11. As desired, the lower bound of μ (μ -LB) stays below unity. However, the upper bound (μ -UB) is higher than unity at the frequency range of the flexible modes. The gap between the μ -LB and -UB can be interpreted as a consequence of the sub-optimality of the algorithms available, and of some conservativeness associated with the adopted LFT. In any case, μ -UB is a sufficient but not necessary condition for robustness, and being close to one is a good indication that robustness is obtained in practice.

The robustness analysis is further matured as follows. For stability robustness, the worst-case (WC) conditions associated with the μ -UB are computed using μ -analysis tools, and simulated in MIL, showing that the system is stable for the considered conditions. For performance robustness, the modulus margin was computed for many realizations of uncertain parameters, showing that -6dB is attained in most configurations, and that all attain a -7dB value, considered compatible with mission objectives.

7.1.2. Post-capture validation

For post-capture, the results for robust stability and performance of μ -analysis are depicted in Figure 11, for the detumbling and pointing controllers. μ -bounds are below one for both controllers, attaining stability and performance-robustness. Similar to pre-capture, the highest μ is attained in the frequencies of the flexible modes. Further physical insight is attained by computing the WC parameters using μ -analysis tools, showing that these correspond to lowest damp factors and frequencies of the flexible modes.

The presented validation results are obtained under the LFT modeling assumptions. Namely, the LFTs consider a subset of most relevant uncertainties and disregard those whose impact is negligible, in order to keep the complexity of the LFT model to a reasonable level and enable the numerical treatability of the problem. For the case of post-capture, chaser mass, chaser inertia matrix, and target mass uncertainty are considered negligible. Also, the operating domain for angular velocity is constrained to 1 deg/s, with the LFT analysis being exceedingly conservative otherwise. High-fidelity MC campaign, that considers to full extent all the effects of closed-loop system, is adopted to resolve the modeling assumptions and limitations found in analytical validation.

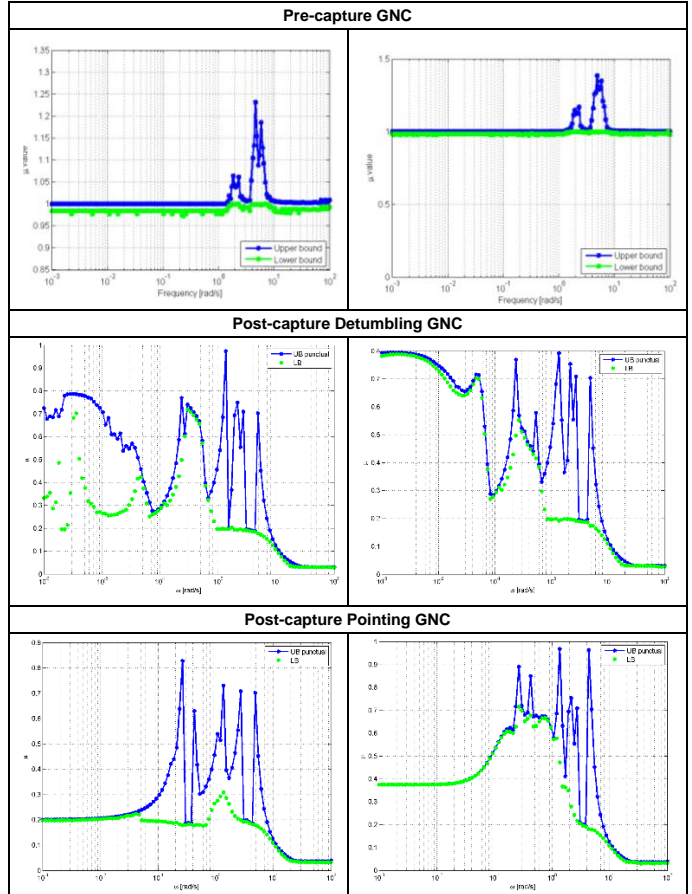


Figure 11 – GNC μ -analysis for stability [left] and performance [right] robustness.

7.2. Time-domain Validation Results

This section presents the results for the MC simulations, that finalize the validation of the robustness and performance requirements defined in Section 2.2. The MC runs are performed accounting for dispersion in all the required model parameters and including all the errors and perturbations. Due to the focus of the paper, other study results are omitted, such as sensitivity analysis with respect to target rotational scenario, relative sensor performance, and specific mission definition parameters, among others.

7.2.1. Pre-capture validation

The validation results for pre-capture are given in Figure 12 for relative position and attitude errors. The sequence of operations is the following: SK until $t=20$ s, SSK until $t=300$ s, SFA until $t=1300$ s, SSK from that time onward.

The analysis of the results shows that robustness and performance requirements are satisfied as follows:

- the GNC accuracy at SK satisfies the 3σ bounds of 20.0cm for position and 2.0cm/s for velocity;

- the GNC accuracy at SSK satisfies the 3σ bounds of 1.2cm for position, 0.5cm/s for velocity, 1 deg for attitude, and 0.1 deg/s for angular velocity;
- the GNC effectively tracks the target pointing;
- the applied actuation is within saturation bounds.

7.2.2. Detumbling and pointing validation

The validation results for detumbling and pointing modes are shown in Figure 13 and Figure 14, respectively, demonstrating that robustness and performance requirements are attained. With respect to performance, the angular velocity stabilizes within the required 3σ bound of 0.1 deg/s, the pointing attitude accuracy is within 3σ bound of 1 deg, and the applied torque actuation is within saturation bounds.

7.2.3. De-orbiting validation

The validation test results for de-orbiting are illustrated in Figure 15, demonstrating that robustness and performance requirements are attained. With respect to performance, the angular velocity and attitude pointing are stabilized with similar performance for all the burns. The attitude errors are below 0.1 deg/s and 1 deg bounds for 99% of the burn duration, which is considered compatible with mission objectives. Commanded control torque is within saturation limits, being able to counteract the torque generated by the 0.1 m slippage of the target CoM w.r.t. chaser main engine axis. The drag torque is also compensated, increasing with the lowering of the perigee, see $t = 4000s$ of the 3rd burn results.

The simulation results also allowed to evaluate aspects such as the clamp load, the fuel consumption, and the maximum height at which the attitude of the composite is controllable by the available torque authority, in the presence of drag torque. The results were according to expected: the clamp structural elements are loaded for the duration of the de-orbit burn; the delta-V is 210.3 m/s; and the minimum controllable height is about 150km.

7.2.4. Assessment of robust control framework

The results obtained in simulation support the robustness results obtained in analytical validation, demonstrating that the modeling assumptions adopted in the analytical validation did not constrain the reliability of the obtained robustness guarantees. This result evidences the benefit of such tools in the design of GNCs with robustness and performance requirements.

8. CONCLUSIONS

This paper presented the development and validation of a GNC for ADR of the ENVISAT S/C using a clamping mechanism. The following steps in the synthesis and analysis

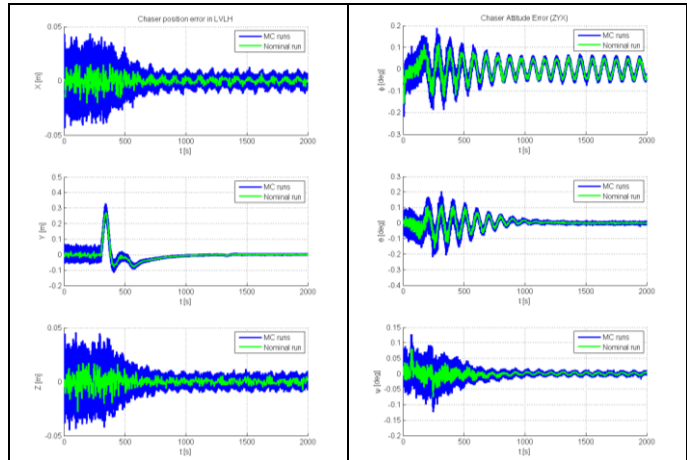


Figure 12 – Pre-capture GNC performance validation: relative position error [left], and attitude error [right].

of the robust MIMO GNC were presented: mission definition and requirements, non-linear system modeling, LFT derivation, GNC design and synthesis for pre- and post-capture phases, and validation in an advanced V&V framework. The presented GNC developments provided the consolidation of a set of requirements and insights that can be considered of interest within the CleanSpace initiative.

9. REFERENCES

- [1] "Space Operations - ESA and Space Debris" brochure, ESA, 2013.
- [2] "e.Deorbit Assessment", ESA CDF study report, 2012.
- [3] "Technical proposal for Rendezvous, capture, detumbling and de-orbiting of an uncooperative target using clamping mechanisms – CLGADR", CLGADR-DME-COM-PCL01-10-E, 2014.
- [4] F. Ankersen, *Guidance, Navigation, Control and Relative Dynamics for Spacecraft Proximity Maneuvers*, PhD Thesis, Aalborg University, Denmark, 2011.
- [5] "e.Deorbit Mission Requirements Document", ESA-ESTEC, 2012.
- [6] Nikravesh, P. E. *Computer-aided analysis of mechanical systems*. Prentice-Hall, Inc., 1988.
- [7] Ibrahim, R. *Liquid Sloshing Dynamics: Theory and Applications*, Cambridge University Press, Cambridge, United Kingdom, 2005.
- [8] Fehse, W., *Automated Rendezvous and Docking of Spacecraft*, Cambridge Aerospace Series, 2003.
- [9] Balas, G.J., Doyle, J.C., Glover, K., Packard, A., Smith, R., " μ -Analysis and Synthesis Toolbox: For Use with MATLAB", 2001.
- [10] "End-Of-Life De-Orbit Strategies Executive Summary", OHB, 2002.
- [11] J. C. Bastante et al., "Design and development of PROBA-3 rendezvous experiment", *Acta Astronautica*, p.311-320, 2013.
- [12] J. C. Bastante et al., "Real Time Real Time Performances of a Vision Based GNC For Automated Rendezvous In Elliptical Orbit", ESA GNC, Karlovy Vary, Czech Republic, 2011.
- [13] Menon, P.P., Prempain, E., Postlethwaite, I., Bates, D.G., "Nonlinear Worst-Case Analysis of an LPV Controller for Approach-Phase of a Re-Entry Vehicle," AIAA GNC, 2009

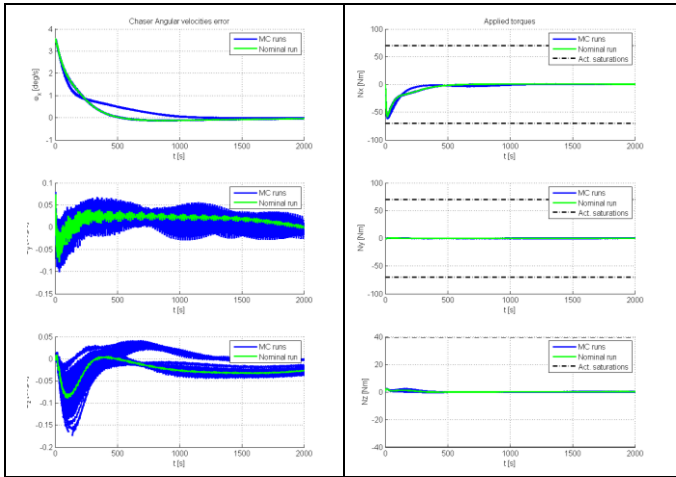


Figure 13 – Detumbling GNC performance validation: angular velocity error [left], and applied torque [right].

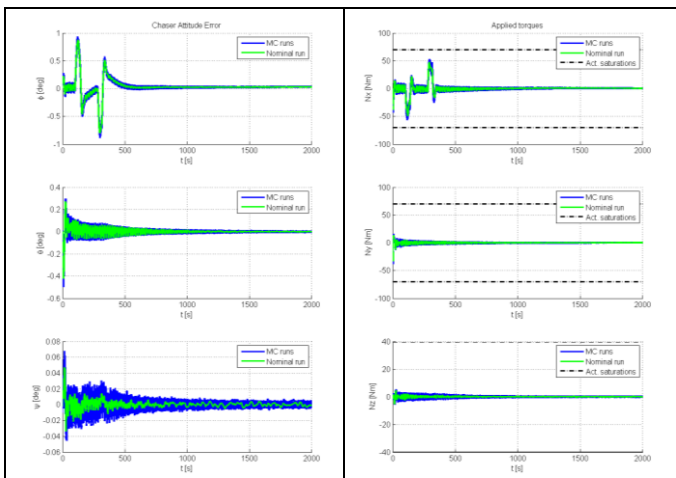
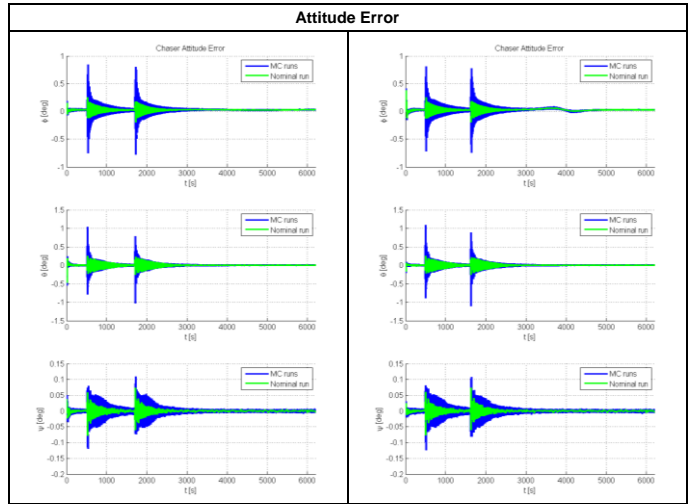


Figure 14 – Pointing GNC performance validation: attitude error w.r.t. Guidance reference [left], and applied torque [right].

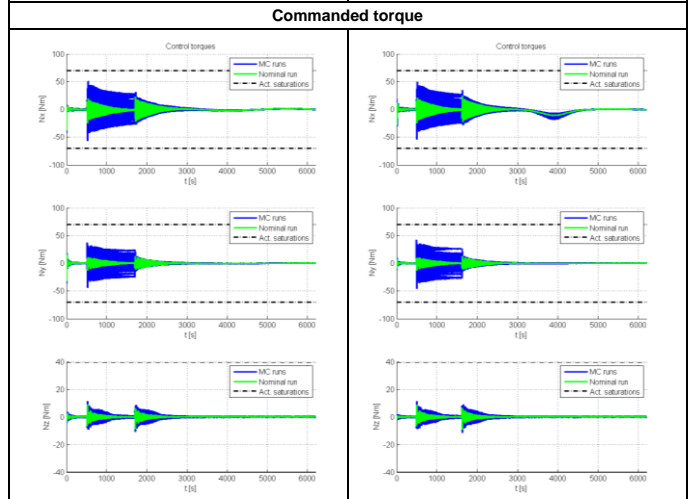
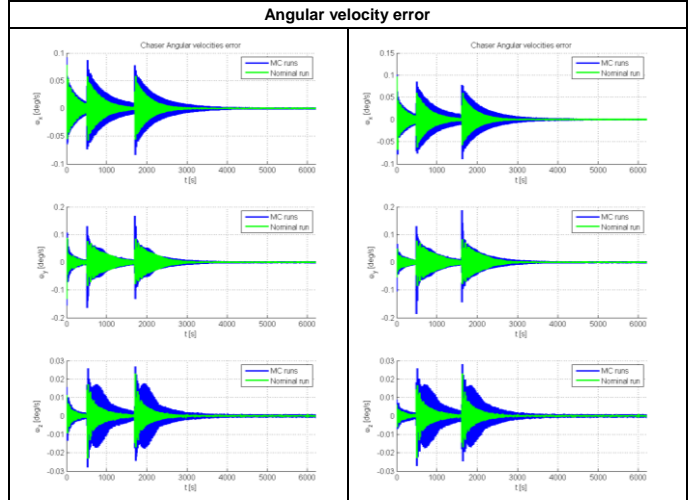


Figure 15 – De-orbit GNC performance validation for 1st burn [left], and 3rd burn [right].